

# Joint statistics of acceleration and vorticity in fully developed turbulence

Luca Biferale<sup>1</sup> and Federico Toschi<sup>2</sup>

<sup>1</sup>Dipartimento di Fisica, Università degli Studi di Roma "Tor Vergata"  
and INFN, Via della Ricerca Scientifica 1, I-00133 Roma, Italy

<sup>2</sup>Istituto per le Applicazioni del Calcolo, CNR,  
Viale del Policlinico 137, I-00161 Roma, Italy

March 28, 2024

## Abstract

We report results from a high resolution numerical study of fluid particles transported by a fully developed turbulent flow at  $Re = 280$ . Single particle trajectories were followed for a time range spanning more than three decades, from less than a tenth of the Kolmogorov time-scale up to one large-eddy turnover time. We present results concerning acceleration statistics and the statistics of trapping by vortex filaments conditioned to the local values of vorticity and enstrophy. We distinguish two different behaviors between the joint statistics of vorticity and centripetal acceleration or vorticity and longitudinal acceleration.

Lagrangian statistic of particles advected by a turbulent velocity field,  $u(x;t)$ , is important both for theoretical implications [1] and for applications, such as the development of phenomenological and stochastic models for turbulent mixing [2,3]. Recently, important advances in experimental techniques for measuring Lagrangian turbulent statistics [4-8] have been achieved. Direct numerical simulations (DNS) also offer very high accuracy albeit at a slightly lower Reynolds number [9-12]. We analyze Lagrangian data obtained from a recent DNS of forced homogeneous isotropic turbulence [17,18], performed on  $512^3$  and  $1024^3$  cubic lattices with Reynolds numbers up to  $Re = 280$ . The Navier-Stokes equations were integrated using fully de-aliased pseudo-spectral methods for a total time  $T = T_L$ . Two millions of Lagrangian particles (passive tracers) were injected into the flow once a statistically stationary velocity field had been obtained. The positions and velocities of the particles were stored at a sampling rate of  $0.07$ . The velocity of the Lagrangian particles was obtained using linear interpolation of the Eulerian field. Acceleration was measured both as the derivative of the particle velocity and by direct computation from all three forces acting on the particle (i.e. pressure gradients, viscous forces and large scale forcing): the two measurements were found to be in very good agreement (with the latter being less noisy). Finally, the flow was forced by keeping the total energy constant in each of the first two wavenumber shells. For more details on the simulation, see [17-19]. Recently much attention focused on the statistics of acceleration with and without conditioning on the local structure of the flow [4,8,16,18,19]. Some phenomenological description of such statistics using multifractal [14,18] or quasi-equilibrium distribution have been also proposed [13] (for a critical summary of these attempts see [15]). In this paper we concentrate mainly on the statistics of trapping events, i.e. those cases when the particle is captured inside a vortex filaments for a time lag considerably larger than the Kolmogorov eddy turnover time, [4,17]. These events contribute to the statistics of the particle acceleration,  $P(a)$ , with extremely intense values, up to 80 times the root mean squares acceleration, at the Reynolds number here investigated (see Fig. 1). In previous analysis [17-19] we have shown that the trapping in vortex filaments is responsible for a strong deterioration of scaling properties of Lagrangian Structure functions for time lags of the order of  $\tau$ . In a previous publication [19] we shown that trapping into vortex filaments leads to very

different dynamical behavior for centripetal and longitudinal acceleration (see also [16]). Being the latter highly oscillating in time, while the former almost constant and with very high amplitude (see Fig. 1). The big difference between the dynamical properties of longitudinal and centripetal acceleration is already detected by inspecting their temporal correlations:

$$C_c(\tau) = \langle a_c^x(t) a_c^x(t+\tau) \rangle / \langle a_c^x(t)^2 \rangle \quad C_l(\tau) = \langle a_l^x(t) a_l^x(t+\tau) \rangle / \langle a_l^x(t)^2 \rangle \quad (1)$$

where we focus only on one component of the acceleration correlation for simplicity. In Fig. 2 we present the DNS results for these two quantities. As one can see, while the longitudinal acceleration decreases with a characteristic time which is comparable with the Kolmogorov time  $\tau_K$ , the centripetal one has a much slower time decay. Indeed, as shown in the inset, the centripetal correlation,  $C_c(\tau)$ , possess two different decays [4,5,16]. The first one, for short time lags (up to  $4\tau_K$ ) is comparable with the one of the longitudinal correlation. The second decay, with a characteristic time of the order of  $10\tau_K$  is established for longer time lags. This second exponential tail is the signature of the strong persistence inside vortex filaments. In order to better quantify this trapping events, we present in this paper some results on the statistical properties of the longitudinal and centripetal acceleration conditioned to the local properties of the vorticity field,  $\omega(x)$  and of the enstrophy,  $E(x)$ . The presence of persistent intense vorticity structure at dissipative scales may have a strong feedback on the energy cascade mechanism. It is not clear if and how these structures may also influence the inertial range physics through non-local effects (filaments are quite elongated in one direction). Other studies similar to the one presented here, but focused on the joint probability distribution of the energy transfer and the vorticity field may help in clarifying this important issue.

## 1 Joint statistics

We want to study the correlation between the probability to observe a large value in the acceleration fluctuations and the local Eulerian structure of the flow. To do that we first define the

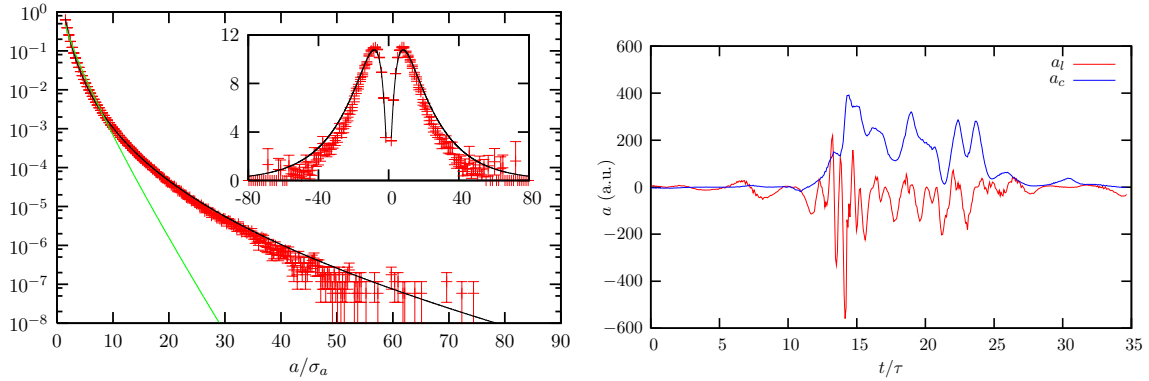


Figure 1: (Left panel). Log-linear plot of the acceleration pdf,  $P(a)$ . The crosses are the DNS data, the solid black line is the multifractal prediction [18] and the green line is the K41 prediction. The statistical uncertainty in the pdf is quantified by assuming that fluctuations grow proportional to the square root of the number of events. Inset: we show  $a^4 P(a)$  to check the statistical convergence up to fourth order moments, the continuous line is the multifractal prediction presented in [18]. (Right panel). We show, in natural units, the behavior of one component of the centripetal and of the longitudinal acceleration. Notice the strong sign persistence of the centripetal acceleration with respect to the longitudinal one.

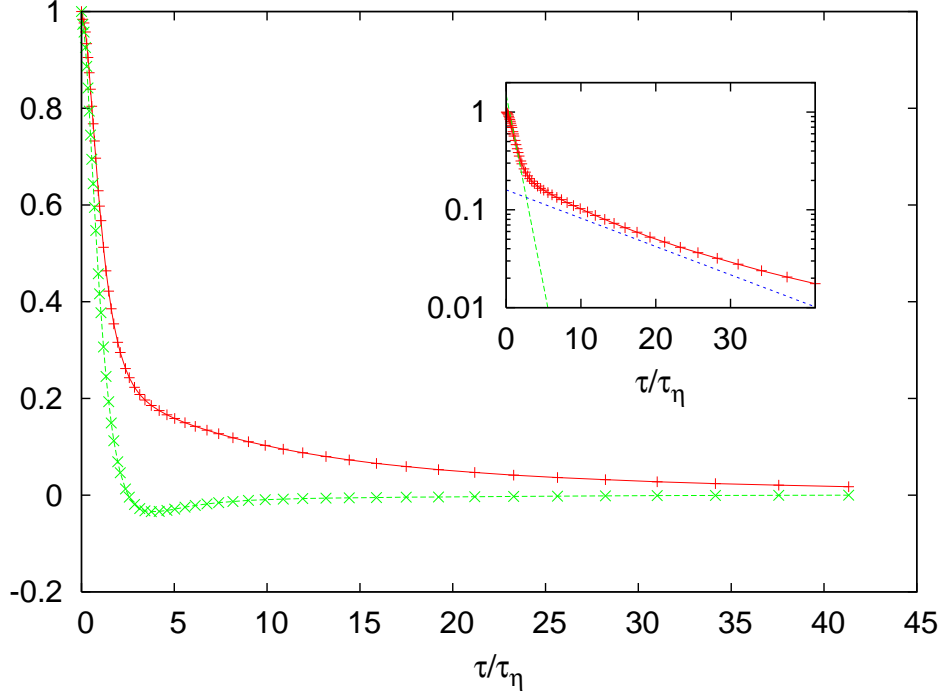


Figure 2: Correlation functions of the centripetal (+, red curve) and longitudinal (? , green curve) accelerations. Notice the much slower decay showed by the centripetal component. Inset: Log-linear plot of the centripetal correlation function,  $C_c(\tau)$ , with superposed the two exponential behavior for short time lags,  $\exp(-\tau/\tau_\eta)$  and for large time lags,  $\exp(-\tau/15\tau_\eta)$ , obtained with a best fit at short and long times respectively.

longitudinal and centripetal instantaneous acceleration to be

$$a_l = (\mathbf{a} \cdot \hat{\mathbf{v}})\hat{\mathbf{v}}$$

and

$$a_c = a - \hat{\mathbf{v}}$$

respectively; where  $\hat{\mathbf{v}}(t)$  is the particle velocity unit vector,  $\mathbf{v}(t) = u(\mathbf{r}(t); t)$ , and  $u(\mathbf{x}; t)$  is the Eulerian velocity field. Similarly, we are interested to the square of the antisymmetric part of the stress tensor, the enstrophy,  $\epsilon(\mathbf{x})$ :

$$\epsilon(\mathbf{x}) = \frac{1}{2} \sum_{ij} (\partial_i v_j - \partial_j v_i)^2 = \frac{1}{2} \omega^2 \quad (2)$$

where  $\omega$  is the vorticity. In a purely circular motion of radius  $r$ , around a vortex filament with vorticity,  $\omega$ , we expect that the centripetal acceleration can be expressed as:

$$|\mathbf{a}_c| = \frac{1}{2} \omega^2 r \quad (3)$$

which is a direct links between the local properties of the enstrophy and the statistics of the centripetal acceleration. The above argument does not fix the  $O(1)$  proportionality prefactor, which depends on the exact shape of the vortex filament. In order to probe how much the rare, but intense, events characterizing the tails of the acceleration statistics are indeed caused by trapping in regions of high vorticity we studied the joint probability densities of centripetal acceleration and

enstrophy, compared with the joint probability density of longitudinal acceleration and enstrophy (for recent similar investigation in experimental and numerical data, see [16]):

$$P(\log(a_c); \log(\epsilon)); P(\log(a_l); \log(\epsilon)) \quad (4)$$

where we concentrate directly with the logarithm of the variable to better appreciate extreme events. Let us first show in Fig. 3 the probability density function of the three (unconditioned) quantities:

$$P(\log(a_c)); P(\log(\epsilon)); P(\log(a_l)):$$

According to relation (3) one would expect that if intense tails in the centripetal acceleration are due to the vortex trapping at Kolmogorov scale, then the two PDF,  $P(\log(\tilde{a}_c))$  and  $P(\log(\epsilon))$  should have the same behavior for large values after the rescaling  $\tilde{a}_c$  is made. This is what we showed in Fig. 3 where one can see that the two tails corresponding to  $P(\log(\tilde{a}_c))$  and to  $P(\log(\epsilon))$  almost perfectly superpose (within  $O(1)$  prefactors which are out of control with dimensional arguments).

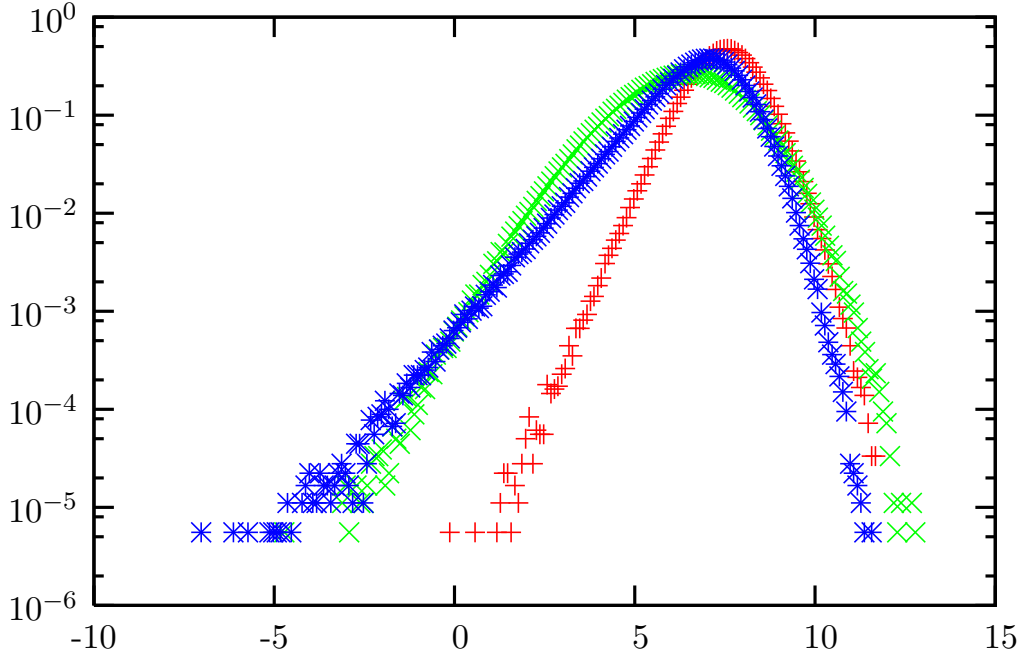


Figure 3: Logarithm of the Probability density function of the instantaneous centripetal acceleration,  $P(\log(\tilde{a}_c))$  (+, red curve), longitudinal acceleration  $P(\log(\tilde{a}_l))$  (? , blue curve) and of the enstrophy,  $P(\log(\epsilon))$  (x, green curve). Acceleration amplitudes are rescaled with the Kolmogorov scale to test relation (3).

However, from the unconditional PDF shown in Fig. 3 there are not strong signs distinguishing the dynamical properties of centripetal and longitudinal acceleration. Similarly, the joint probability densities (4) plotted in Fig. 4 do not show any quantitative differences between the statistics of the centripetal and longitudinal acceleration. This is quite natural, because the motion of a particle in a turbulent field will be characterized by different accelerations and decelerations, not necessarily associated with spiraling motion (on average the mean value of the acceleration will be zero). The distinguishing character of vortex trapping is the strong persistence of the direction- and amplitude- of the centripetal acceleration for time lags much larger than  $\tau_\eta$ , at variance with what happens to the longitudinal acceleration, see right panel of Fig. 1.

To make this statement quantitative, we have studied the running average of the centripetal

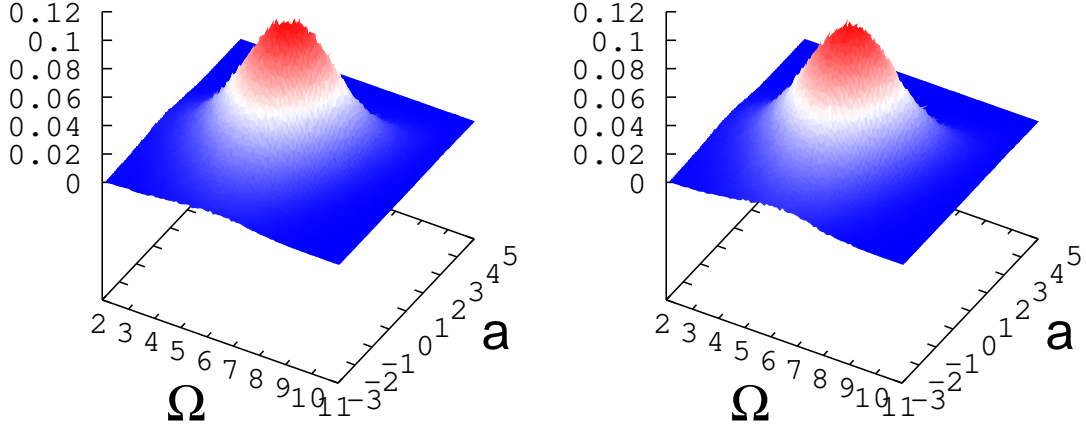


Figure 4: Joint probability distribution function for one component of the centripetal acceleration and enstrophy,  $P(\log(a_c^x); \log(\Omega))$  (Left panel), and of longitudinal acceleration and enstrophy  $P(\log(a_l^x); \log(\Omega))$  (Right panel). Notice that the two shapes are almost indistinguishable.

and longitudinal acceleration, over a time window varying up to 10 [19]:

$$a_c(t) = \frac{1}{Z_{t^0, t^0+2}} \int_{t^0}^{t^0+2} dt^0 a_c(t^0); \quad (5)$$

$$a_l(t) = \frac{1}{Z_{t^0, t^0+2}} \int_{t^0}^{t^0+2} dt^0 a_l(t^0); \quad (6)$$

We expect that the pdfs of the averaged centripetal and longitudinal acceleration will behave very differently at increasing the window size,  $\Delta t$ . In particular, the strong persistence of the centripetal acceleration up to 10 suggests that the joint PDF of centripetal acceleration and enstrophy,  $P(\log(a_c); \log(\Omega))$  should remain almost unchanged at varying  $\Delta t$ , while the longitudinal one  $P(\log(a_l); \log(\Omega))$  should experience a strong depletion, of events with simultaneous intense values of acceleration and vorticity.

A way to offer a quantitative measurement of the correlation between the two variables entering the joint PDF,  $P(x; y)$ , is to plot the residual value,  $R(x; y) = P(x; y) - P(x)P(y)$ , obtained by subtracting the probability density in the case of fully uncorrelated variables,  $P(x)P(y)$ . This is what we show in Figs. (5-6) where we compare the residual value for the averaged centripetal acceleration and the local enstrophy:

$$R(\log(a_c); \log(\Omega)) = P(\log(a_c); \log(\Omega)) - P(\log(a_c))P(\log(\Omega)) \quad (7)$$

and the same quantity for the longitudinal one:

$$R(\log(a_l); \log(\Omega)) = P(\log(a_l); \log(\Omega)) - P(\log(a_l))P(\log(\Omega)) \quad (8)$$

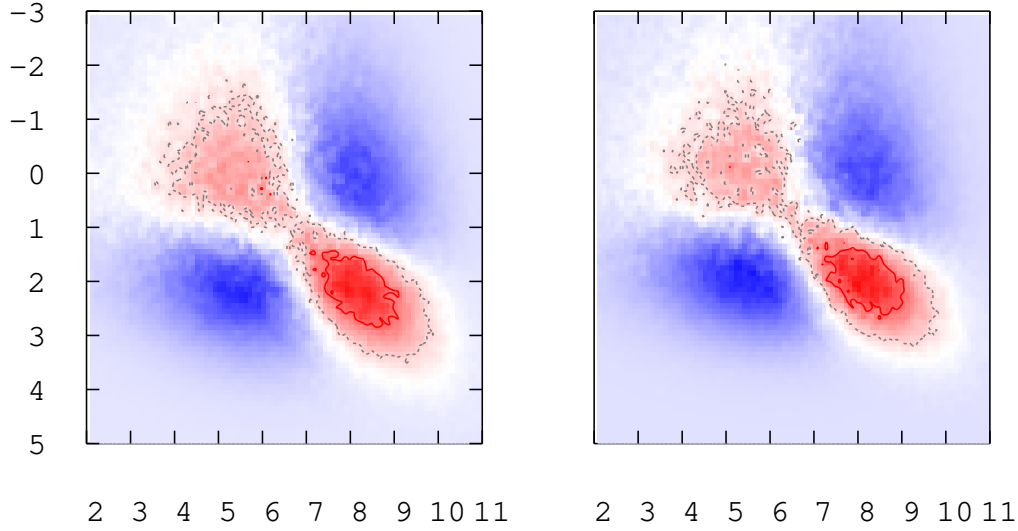


Figure 5: (Left panel). Residual value,  $R(\log(a_c); \log(\epsilon))$  for the centripetal acceleration and the local enstrophy without any average in time (i.e.  $\tau = 0$ ). Acceleration is plotted on the y axis while the enstrophy is plotted on the x axis. (Right panel). The same but for the longitudinal acceleration,  $R(\log(a_l); \log(\epsilon))$ . The isoline is drawn for a fixed value of  $R$ , to guide the eyes. Notice the strong correlation between intense vorticity events and intense centripetal and longitudinal acceleration (bottom right corner). Without averaging in time, no clear distinction between longitudinal and centripetal signal can be detected. As expected, the distinction arises only when persistent effects are investigated, see Figure (6).

for two different values of the window,  $\tau$ . Let us stress that the difference from zero of the residual values here defined give a direct measurement of the level of correlation between the two fluctuating quantities. Positive values of the difference in (7) and (8) indicate correlation while negative values indicate anti-correlation. In Fig. 5 we plot the case of (no-average in time)  $\tau = 0$ , and in Fig. 6 the case of  $\tau = 9$ . As one can see, in the first case, (Fig. 5), a strong correlation between extreme events in the acceleration and the vorticity is observed, although almost no difference is detectable between the longitudinal and centripetal acceleration (right and left panels, respectively). On the other hand, once averaged in time, i.e. filtering out the high oscillation in the longitudinal acceleration, a strong peak in the acceleration-vorticity contour plot is visible only for the centripetal case (see left panel of Fig. 6). This is in our view a simple but effective way to highlight the strong correlation between the observed high tails in the acceleration distribution and the presence of vortex filaments in the Eulerian field.

## 2 Conclusions

We have presented results on the joint Lagrangian acceleration statistics and Eulerian vorticity field from DNS of fully developed turbulence. In particular we have shown the existence of strong

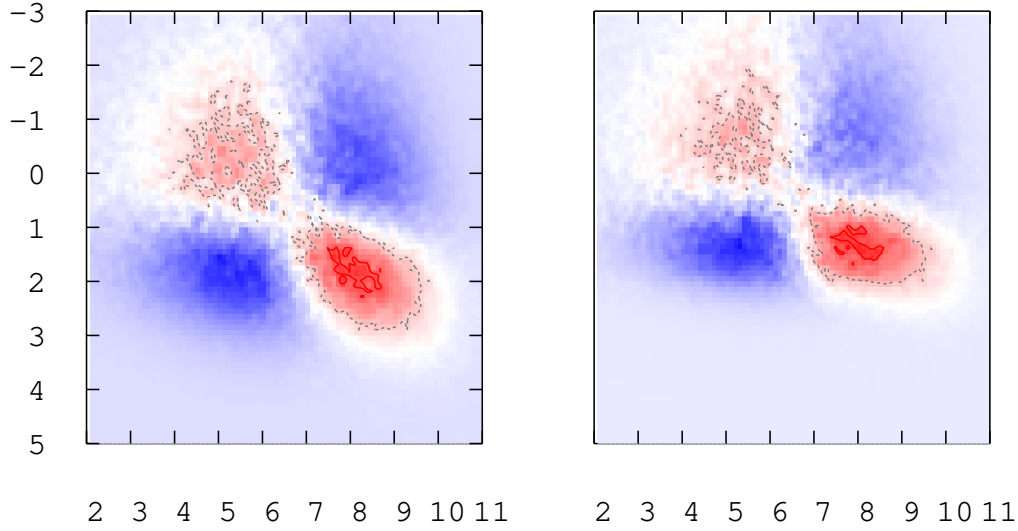


Figure 6: (Left panel). Residual value,  $R(\log(a_c); \log(\epsilon))$ , for the centripetal acceleration and the local enstrophy after averaging in time, over a window  $\Delta t = 9$ . (Right panel). The same but for the longitudinal acceleration,  $R(\log(a_l); \log(\epsilon))$ . The isoline is drawn for a fixed value of  $R$ , to guide the eyes. Notice the persistence of the strong correlation present between intense vorticity events and intense centripetal acceleration. On the other hand, now the longitudinal acceleration is not anymore correlated for intense events with the enstrophy (compare the bottom right corners of both panels).

correlation between intense and persistent centripetal acceleration and the presence of intense vortical structure. No effects similar to this one is detected for the longitudinal components of the acceleration. We interpret this as an evidence of particle trapping in vortex filaments. Further investigations are necessary in order to understand if and how this event affects the local energy transfer mechanism and, if it is the case, how to include the presence of these elementary structure in the energy cascade phenomenology.

We thank G. Boffetta, A. Celani, B. Devenish and A. Lanotte for discussions. We thank the supercomputing center CINECA (Bologna, Italy) and "Centro Ricerche e Studi Enrico Fermi" for the resources allocated for this project. We acknowledge Dr. Nazario Tantalò for technical assistance.

## References

## References

- [1] Kraichnan RH 1965 Phys. Fluids 8 575.
- [2] Pope SB 2000 Turbulent Flows (Cambridge University Press, Cambridge).

- [3] Aringazin AK and Mazhitov MI 2003 Phys. Lett. A 313 284. Aringazin AK and Mazhitov MI 2004 Phys. Rev. E 70, 036301.
- [4] La Porta A, Voth GA, Crawford AM, Alexander J and Bodenshatz E 2001 Nature 409 1017. Voth GA et al 2002 J. Fluid Mech. 469 121. Mordant N et al. 2003 Physica D 193 245.
- [5] Mordant N et al. 2003 J. Stat. Phys. 113 701. Mordant N et al. 2002 Phys. Rev. Lett. 89 254502. Mordant N et al. 2001 Phys. Rev. Lett. 87 214501.
- [6] Ott S and Mann J 2000 J. Fluid Mech. 422 207.
- [7] Chevillard L, Roux SG, Leveque E et al. 2003 Phys. Rev. Lett. 91 214502.
- [8] A.M. Crawford, N. Mordant and E. Bodenschatz 2005 Phys. Rev. Lett. 94, 024501.
- [9] Yeung PK 2002 Ann. Rev. Fluid Mech. 34 115. Yeung PK 2001 J. Fluid Mech. 427 241. Vedula P and Yeung PK 1999 Phys. Fluids 11 1208.
- [10] Yeung PK and Borgas M 2004 J. Fluid Mech. 503 93.
- [11] Boetta G. and Sokolov IM 2002 Phys. Rev. Lett. 88 094501.
- [12] Ishihara T and Kaneda Y 2002 Phys. Fluids 14 L69.
- [13] Beck C 2003 Europhys. Lett. 64 151. Beck C 2001 Phys. Lett. A 27 240.
- [14] Arimitsu T and Arimitsu N 2003 Physica D 193 218.
- [15] Gotoh T and Kraichnan RH 2004 Physica D 193 231.
- [16] Mordant N, Leveque E and Pinton JF 2004 New J. Phys. 6 116.
- [17] Biferale L, Boetta G, Celani A, Lanotte A and Toschi F 2005 Phys. Fluids 17 021701.
- [18] Biferale L, Boetta G, Celani A, Devenish BJ, Lanotte A and Toschi F 2004 Phys. Rev. Lett. 93 064502.
- [19] Biferale L, Boetta G, Celani A, Devenish BJ, Lanotte A and Toschi F 2004 Jour. of Turbulence to appear (2005); [arXiv.org/nlin.CD/0501041](http://arXiv.org/nlin.CD/0501041)